Sn-Bridged Au–Au Interactions

Gold–Gold Interaction—Stannaborate $[SnB_{11}H_{11}]^{2-}$ Coordination Chemistry**

*Siegbert Hagen, Ingo Pantenburg, Florian Weigend, Claudia Wickleder, and Lars Wesemann**

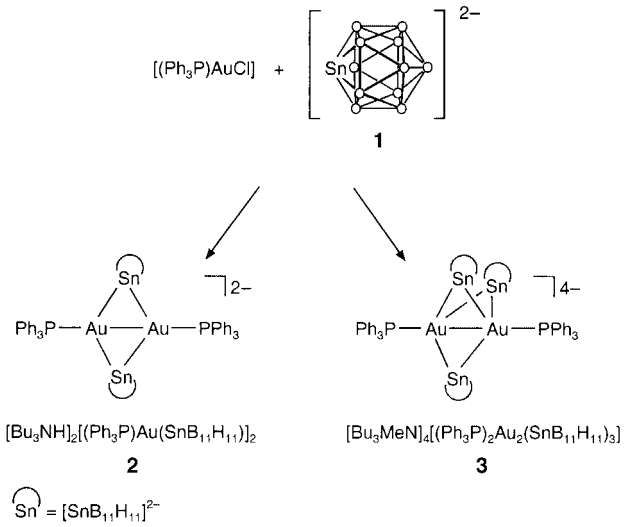

Scheme 1. Reaction of stanna-*closo*-dodecaborate $[SnB_{11}H_{11}]^{2-}$ (**1**) with the gold complex $[(Ph_3P)AuCl]$.

We are currently investigating the coordination chemistry and ligand properties of the dianionic stanna-*closo*-dodecaborate cluster $[SnB_{11}H_{11}]^{2-}$ (**1**). So far, in a variety of transition-metal complexes, the ligand was found to coordinate exclusively as a terminal ligand with the formation of a tin–metal bond.[1]

Here we present the surprising results of preliminary investigations on the stannaborate chemistry with gold electrophiles. Two different gold–tin clusters $[Bu_3NH]_2[(Ph_3P)Au(SnB_{11}H_{11})]_2$ (**2**) and $[Bu_3MeN]_4[(Ph_3P)_2Au_2(SnB_{11}H_{11})_3]$ (**3**) (Scheme 1), which were characterized by NMR spectroscopy, elemental analysis, and X-ray crystal structure analysis, were isolated from equimolar mixtures of **1** and the gold complex $[(Ph_3P)AuCl]$ depending on the counterion of the stannaborate.

^{31}P NMR spectra (recorded at 213 K) reveal that the different countercations $[Bu_3NH]^+$ or $[Bu_3MeN]^+$ have no influence on the composition of the 1:1 reaction mixture ($[SnB_{11}H_{11}]^{2-}$:$[(Ph_3P)AuCl]$). Interestingly, 50% of the starting material $[(Ph_3P)AuCl]$ is still present in the mixture. The other signals in the ^{31}P NMR spectrum exhibit tin satellites, which provides direct spectroscopic evidence for the formation of a covalent Au–Sn bond. In this solution the anion of **3** is the major Au–Sn component (35%) and exhibits a characteristic signal in the ^{31}P NMR spectrum at $\delta =$ 54.4 ppm with a $^2J(Sn,P)$ coupling constant of 109.4 Hz. The anion of **2** was identified in solution by a small signal (3%) at $\delta = 62.9$ ppm ($^2J(Sn,P) = 186.9$ Hz). A bis(triphenylphosphane) substitution product ($[(Ph_3P)_2Au(SnB_{11}H_{11})]^-$) is also present in solution (5%) and displays a signal in the ^{31}P NMR spectrum at $\delta = 44.5$ ppm ($^2J(P,^{117}Sn) = 984.2$ Hz, $^2J(P,^{119}Sn) =$ 1027.5 Hz). This compound was synthesized in a separate experiment from nucleophile **1**, PPh_3, and $[(Ph_3P)AuCl]$ in reasonable yield and details will be published later. Treatment of the $[(Ph_3P)AuCl]$ with 1.5 equivalents of heteroborate **1**, led to an increase in the amount of Au_2Sn_3 cluster **3** formed (68.6% yield).

The geometry of the metal core in the anions of **2** (Figure 1) and **3** (Figure 2) shows a surprising correspondence with the respective arrangements in $[Au_2Pt_2(PPh_3)_4(CN\text{-}xylyl)_4]^{2+}$ [2] and the trigonal bipyramid in $[(Ph_3P)_2Pt_2\{Sn(acac)_2\}_3]$ (acac = acetylacetonate).[3]

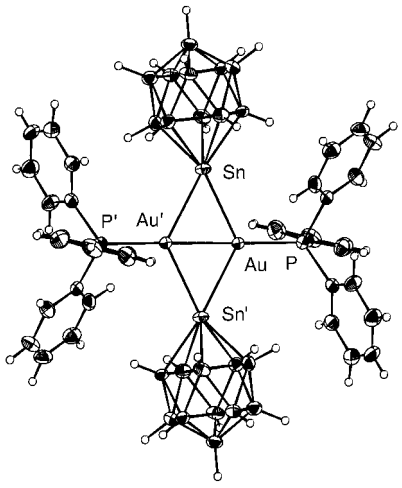

Figure 1. Molecular structure of the anion of **2** in the solid state; the dianion lies on the center of symmetry. Interatomic distances [pm] and angles [°]: Au-Sn 273.7(1), Au′-Sn 276.1(1), Au-Au′ 262.5(1), Au-P 233.2(1); P-Au-Au′ 178.78(4), P-Au-Sn 116.86(3), P-Au-Sn′ 120.17(3), Au-Sn-Au′ 57.03(1), Au-Au′-Sn 61.95(2).

[*] Prof. Dr. L. Wesemann, S. Hagen, Dr. I. Pantenburg, Dr. C. Wickleder
Institut für Anorganische Chemie
Universität zu Köln
Greinstrasse 6, 50939 Köln (Germany)
Fax: (+49) 221-470-4899
E-mail: lars.wesemann@uni-koeln.de
Dr. F. Weigend
Institut für Nanotechnologie
Forschungszentrum Karlsruhe
Postfach 3640, 76021 Karlsruhe (Germany)

[**] This work was supported by the Deutsche Forschungsgemeinschaft (DFG-Schwerpunktprogramm "Polyeder").

 DOI: 10.1002/ange.200250698

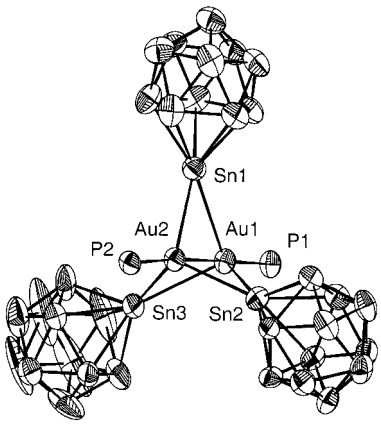

Figure 2. Molecular structure of the anion of **3** in the solid state. Hydrogen atoms and phenyl substituents have been omitted for clarity. Interatomic distances [pm] and angles [°]: Au1-Au2 259.0(1), Au1-Sn1 272.7(1), Au1-Sn2 271.1(1), Au1-Sn3 271.8(1), Au1-P1 231.5(2), Au2-Sn1 294.7(1), Au2-Sn2 303.2(1), Au2-Sn3 298.0(1), Au2-P2 230.1(2); P1-Au1-Au2 176.56(6), P2-Au2-Au1 179.05(6), P1-Au1-Sn1 111.22(6), P1-Au1-Sn2 108.45(6), P1-Au1-Sn3 115.31(6), P2-Au2-Sn1 121.57(6), P2-Au2-Sn2 122.24(6), P2-Au2-Sn3 122.72(6), Au1-Sn1-Au2 54.23(2), Au1-Sn2-Au2 53.26(2), Au1-Sn3-Au2 53.76(2), Sn1-Au1-Sn2 111.71(2), Sn1-Au1-Sn3 105.79(2), Sn2-Au1-Sn3 104.19(2), Sn1-Au2-Sn2 97.44(2), Sn1-Au2-Sn3 94.24(2), Sn2-Au2-Sn3 91.08(2).

The most striking features in the gold–tin clusters **2** and **3** are the novel bridging mode of the stannaborate ligand and the short Au–Au interatomic distance. Tin ligands bridging two transition metal centers are well known;[4] for example, the tetrahedral gold cluster $[Au_4(PPh_3)_4(\mu_2\text{-}SnCl_3)_2]$, in which two of the Au–Au edges are bridged by the $SnCl_3$ groups, was presented by Mingos et al. as the first example of μ_2-$SnCl_3$ coordination.[5] In **2** we find a nearly symmetrically μ_2-coordinated heteroborate; the Au–Sn distances are 276.1(1) and 273.7(1) pm. Owing to steric crowding in the tetraanion of **3**, the three heteroborates are unsymmetrically bonded to the Au–Au edge with three shorter distances to Au1 (271.1(1)–272.7(1) pm) and three very long contacts to Au2 (294.7(1)–303.2(1) pm). The short Au–Sn distances in **2** and **3** are in the middle of the range of known Au–Sn bond lengths (256.5(1)–297.3(8) pm),[5–10] whereas the longer Au–Sn distances in **3** can be compared with the respective bond lengths in $[Au_4(PPh_3)_4(\mu_2\text{-}SnCl_3)_2]$ (281.5(7), 297.3(8) pm) and are indicative of weak interactions between the ligand and the Au2 atom in the solid state.[10] Although gold chemistry is one of the most active fields of research, very few compounds bearing Au–Sn bonds are known.[11]

Au–Au bond formation has been studied extensively and the short Au–Au distances (262.5(1) and 259.0(1) pm) in **2** and **3** suggest strong metal–metal interactions.[12] Formally, we find Au^I in clusters **2** and **3**, but the Au–Au bond lengths are shorter than the discussed values for Au^I–Au^I interactions (275–325 pm).[12] In both **2** and **3** the P-Au-Au-P axis is linear, and this geometry together with the short Au–Au bonds can be compared with those in the heteroatomic gold clusters $[(dppe)_2Au_3In_3Cl_6(thf)_3]$ (dppe = 1,2-bis(diphenylphosphanyl)ethane),[13] $[(dppe)_2Au][(dppe)_2Au_3In_3Br_7(thf)]$,[14] $[Au_4(PPh_3)_4(\mu_2\text{-}SnCl_3)_2]$,[5] $[Au_2Pt_2(PPh_3)_4(CN\text{-}xylyl)_4]$,[2] and $[Au_4(PPh_3)_4(\mu_2\text{-}I)_2]$.[15] On the basis of these findings and in agreement with the situation in Au_3In_3 clusters, an oxidation state of zero can be considered for the gold atoms in **2** and **3**.[13,14]

Quantum-chemical calculations[16] have been carried out for the anion of **2**. This dianion might be regarded as a dimer consisting of two $[(Ph_3P)Au(SnB_{11}H_{11})]^-$ units. Such a monomer could be expected to be quite stable, since the Au atom in this case would be linearly coordinated by the ligands, which often is preferred by Au due to relativistic effects.[17] We initially calculated the stability of the dimer to fragmentation into monomers, that is, the energy difference between the dimer and two monomers in optimized geometries, and then we investigated the interactions that are responsible for the stability of the dimer.

Results obtained with DFT[18] (B-P functional[19,20]), HF, and HF + MP2 calculations[21] were compared; to keep computational effort moderate, Ph_3P was replaced by Me_3P throughout, and in the MP2 calculations orbitals with energies below −100 eV were neglected (frozen core). The description of anionic species requires the use of flexible basis sets; we used TZVP-quality basis sets for the DFT calculations, whereas we used TZVPP-type basis sets for Au, Sn, P, and S and SV(P)-type basis sets for B, C, and H for the HF and the MP2 calculations,[22] in case of Au (Sn) the inner 60 (46) electrons were represented by effective core potentials, which also include scalar relativistic effects.[23] With these basis sets we obtained negative values for the HOMO at the HF level: −3.2 eV for the dimer, −4.6 eV for the monomer (smaller basis sets might lead to positive values corresponding to unbound states). Moreover one might suspect, that due to its higher charge, the dimer is not described as well as the monomer. To estimate this effect single-point DFT calculations were performed for compounds in which both anions were embedded in a metallic environment;[24] in this way the negative charges are compensated by positive image charges.

A significant preference of the dimer over the two monomers is observed only at the HF + MP2 level (ΔE = 160 kJ mol^{-1}). This is not observed for the DFT calculations (+4 kJ mol^{-1}), even if the anion is embedded in a metallic environment (+23 kJ mol^{-1}). At the HF level the dimer is even disadvantaged (−50 kJ mol^{-1}); moreover, at this level it is not a minimum structure, since calculation of the vibration spectrum yields two imaginary modes. These large differences can be attributed to the different treatment of dynamical electron correlation at each level. In the case of HF it is neglected, at the DFT level it is modeled by an exchange-correlation functional of the electronic density, and MP2 accounts for it by means of perturbation theory applied to the HF wave function; only the latter method explicitly includes the description of dispersive interactions, which are clearly relevant for the stability of the dimer. This is also evident from the Au–Au and Au–Sn distances, which are accurately described only at the HF + MP2 level (denoted "full" MP2 in Table 1); differences to the experimental values are negligible, −1 pm to +2 pm. At the DFT (HF) level errors are much larger; Sn–Au distances are overestimated by about 13 (17) pm, for the Au–Au distance the difference is less pronounced, +3 (+9) pm.

Table 1: Distances obtained at different levels of theory. In the case of MP2, the groups of orbitals that were included in the treatment are given in the second column (see also Figure 3).

	Correlated electrons	Au–Au [ppm]	Sn–Au [ppm]
experiment		263	274–276
DFT	(all)	266	287–288
HF	(none)	272	292–293
"full" MP2	I–V + 4p(Au) ($\varepsilon > -100$ eV)	262	274
MP2	III	262	285–286
MP2	V	272	293
MP2	III + V	262	276

As in previous work,[25] the following procedure was used to determine whether particular electrons are in any way responsible for the binding correlation effects. Figure 3 shows the density of states (DOS), which results from the HF wave function[26] in the MP2 geometry. Contributions of different parts of the molecule to the DOS were calculated by a Mulliken population analysis for each orbital and are also

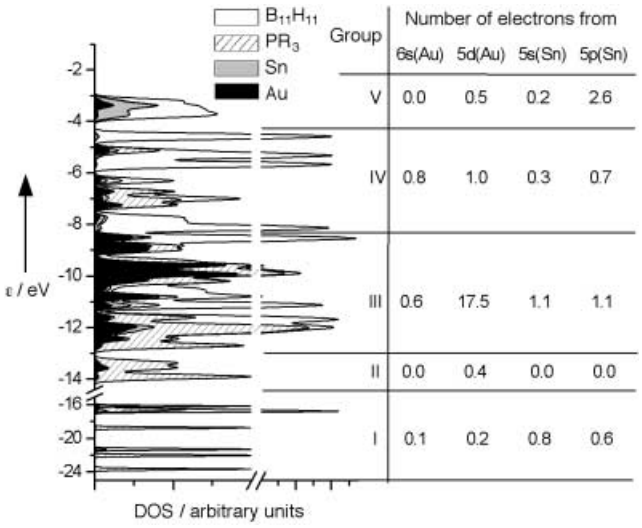

Figure 3. Density of states resulting from a Mulliken population analysis of the HF wave function in the MP2 geometry for $[(Ph_3P)Au(SnB_{11}H_{11})]_2^{2-}$. Orbital energies are superimposed by Gauss functions of width = 0.1 eV to help the eye. Contributions from different parts of the system are indicated; at the right-hand side contributions of the valence electrons of Sn and Au are listed separately.

displayed in Figure 3. Orbitals thus may be partitioned into groups. Groups I, II, and V are energetically separated from groups III and IV, group III was regarded as separated from group IV, because group III contains the main contribution from the 5d(Au) electrons, whereas their contribution to group IV is very small; 5p(Sn) electrons are mainly found in group V.

In the next step geometry optimizations at the HF + MP2 level were performed in which only electrons from some of the groups in the MP2 treatment were included; the resulting bond lengths are displayed in Table 1. Mulliken population analyses were also carried out for the optimized geometries, and the results were very similar to that shown in Figure 3, which indicates that changes in orbital characteristics are rather small.

Including only electrons of group III (5d(Au)) is sufficient to obtain an Au–Au distance very similar to that from the full MP2 treatment; the Sn–Au distances are 6 pm shorter than those calculated at the HF level (probably because there are also small contributions from the Sn atoms in group III), but still 10 pm longer than the value determined from the full MP2 treatment. Including only electrons from group V (p(Sn)) in the MP2 treatment yields results very similar to those from the HF calculation; but when electrons from group III and V are included, the Sn–Au and Au–Au distances are nearly the same as those determined in the full MP2 calculation. This indicates that the stability of the dimer over two monomers is predominantly due to dispersive interactions between the valence electrons of both Sn and Au.

Finally we confirmed the assignment of an oxidation state of 0 for the gold atom. Mulliken population analyses of the HF and the (HF + MP2) density yield charges of 0.15 (0.028) electrons for the Au atom; values in Au^I compounds are significantly larger (e.g. Au_2S: 0.41 (0.23)).

The luminescence of many polynuclear gold complexes has attracted considerable attention.[27,28] The Au_2Sn_3 cluster **3** luminesces in the solid state and displays an intense red emission at low temperatures upon excitation in the UV range (Figure 4).

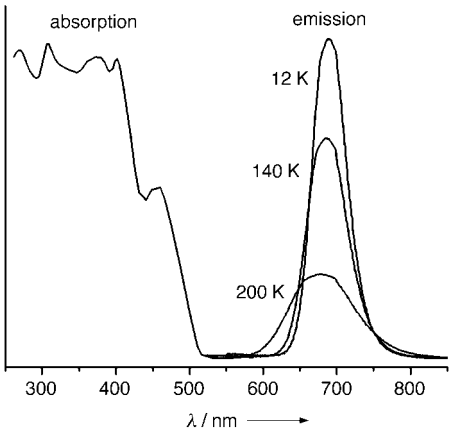

Figure 4. Temperature-dependent emission spectra of **3**. The absorption spectra was recorded at 12 K.

At 12 K the maximum of the emission is located at 690 nm (14490 cm^{-1}) with $\Delta_{1/2} = 1150$ cm^{-1}. Thermal excitation of the vibrational levels of the electronic excited state causes a blue shift of the maximum, and an increase of the band width occurs on increasing the temperature (200 K: $\lambda_{max} = 679$ nm, $\nu_{max} = 14732$ cm^{-1}, $\Delta_{1/2} = 2328$ cm^{-1}). Temperature-dependent lifetime measurements were performed on the excitation at 355 nm (8 ns pulse) and on the emission at 690 nm: $\tau =$ 138.4 μs at 12 K; $\tau = 10.2$ μs at 240 K (single exponential decay).

In conclusion, coordination of the tin nucleophile at Au^I centers results in signifcant gold–gold interaction and reduction of the oxidation state to Au^0.[29]

Experimental Section

2: Treatment of [(Ph$_3$P)AuCl] (151 mg, 0.31 mmol) in CH_2Cl_2 (15 mL) at room temperature with a solution of $[Bu_3NH]_2[SnB_{11}H_{11}]$ (185 mg, 0.3 mmol) in CH_2Cl_2 (15 mL) led to an orange solution. After the mixture had been stirred for 1 h, volatiles were removed in vacuum and the residue was washed with water. Crystallization by slow diffusion of hexane into a solution of the crude product in CH_2Cl_2 afforded **2** (166 mg, 31% yield) as colorless crystals. ^{11}B {^{1}H} NMR: $\delta = -14.5$ ppm; ^{31}P {^{1}H} NMR: $\delta = 62.9$ ppm (^2J(Sn,P) = 186.9 Hz); elemental analysis (%) calcd: C 40.29, H 6.09, N 1.57; found: C 39.15, H 5.54, N 1.61.

3: Treatment of [(Ph$_3$P)AuCl] (148 mg, 0.3 mmol) in CH_2Cl_2 (15 mL) at room temperature with a solution of $[Bu_3MeN]_2[SnB_{11}H_{11}]$ (292 mg, 0.45 mmol) in CH_2Cl_2 (20 mL) led to an orange solution. After the mixture had been stirred for 1 h, volatiles were removed in vacuum and the residue was washed with water. Crystallization of the crude product from a mixture of CH_2Cl_2/hexane at room temperature afforded **3** (218 mg, 59% yield with respect to tin ligand) as pale yellow crystals. ^{11}B {^{1}H} NMR: $\delta = -14.1$ ppm; ^{31}P {^{1}H} NMR: $\delta =$ 54.4 ppm (^2J(Sn,P) = 109.4 Hz); ^{119}Sn {^{1}H} NMR: $\delta = -332$ ppm; elemental analysis (%) calcd: C 42.86, H 7.48, N 2.27; found: C 42.68, H 7.74, N 2.31.

Single-crystal structure determination: The intensity data were collected on an imaging-plate diffractometer (IPDSII, Stoe & Cie) with $Mo_{K\alpha}$ radiation ($\lambda = 71.073$ pm, graphite monochromator) at 170 K. Several C atoms of the cations in **3** show large thermal displacement factors. Therefore, these atoms were refined isotropically by using a split model without consideration of the H atoms.[30–33] All of the other non-hydrogen atoms were refined with anisotropic temperature factors. The hydrogen-atom positions for **2** were taken from the difference Fourier map at the end of the refinement. The hydrogen atoms for **3** are in calculated positions.

Crystal data for **2**: $C_{60}H_{108}B_{22}N_2P_2Sn_2Au_2$, triclinic space group $P\bar{1}$, $a = 1075.0(1)$, $b = 1181.8(2)$, $c = 1623.6(2)$ pm, $\alpha = 74.45(1)$, $\beta = 85.80(1)$, $\gamma = 68.97(1)°$, $Z = 1$, $\mu = 4.691$ mm^{-1}; $F(000) = 880$, $R_{int} = 0.0493$, no. collected/unique/$I_0 > 2\sigma I_0$ data = 21 407/9869/6623, $R1/wR2$ (all data) = 0.0672/0.0618, $R1/wR2$ ($I_0 > 2\sigma I_0$) = 0.0348/0.0552, max./min. electron density = $1.42/-2.11 \times 10^{-6}$ e pm^{-3}.

Crystal data for **3**: $C_{88}H_{183}B_{33}N_4P_2Sn_3Au_2$, monoclinic space group $P2_1/c$, $a = 2607.5(1)$, $b = 1699.0(1)$, $c = 2806.5(1)$ pm, $\beta = 106.47(1)°$, $Z = 4$, $\mu = 3.139$ mm^{-1}; $F(000) = 4968$, $R_{int} = 0.1062$, no. of collected/unique/$I_0 > 2\sigma I_0$ data = 109 394/20 724/14 474, $R1/wR2$ (all data) = 0.0863/0.1359, $R1/wR2$ ($I_0 > 2\sigma I_0$) = 0.0589/0.1299, max./min. electron density = $2.09/-1.12 \times 10^{-6}$ e pm^{-3}.

CCDC-198734 (**2**) and CCDC-198733 (**3**) contain the supplementary crystallographic data for this paper. These data can be obtained free of charge via www.ccdc.cam.ac.uk/conts/retrieving.html (or from the Cambridge Crystallographic Data Centre, 12, Union Road, Cambridge CB21EZ, UK; fax: (+44) 1223-336-033; or deposit@ccdc.cam.ac.uk).

Received: December 4, 2002 [Z50698]

Keywords: ab initio calculations · boranes · cluster compounds · gold · tin

[1] a) L. Wesemann, S. Hagen, T. Marx, I. Pantenburg, M. Nobis, B. Drießen-Hölscher, *Eur. J. Inorg. Chem.* **2002**, 2261 – 2265; b) T. Marx, L. Wesemann, S. Dehnen, I. Pantenburg, *Chem. Eur. J.* **2001**, *7*, 3025 – 3032.

[2] C. E. Briant, D. I. Gilmour, D. M. Mingos, *J. Organomet. Chem.* **1984**, *267*, C52 – C55.

[3] G. W. Bushnell, D. T. Eadie, A. Pidcock, A. R. Sam, R. D. Holmes-Smith, S. R. Stobart, E. T. Brennan, T. S. Cameron, *J. Am. Chem. Soc.* **1982**, *104*, 5837 – 5839.

[4] a) W. Petz, *Chem. Rev.* **1986**, *86*, 1019 – 1047; b) M. S. Holt, W. L. Wilson, J. H. Nelson, *Chem. Rev.* **1989**, *89*, 11 – 49; c) D. J. Cardin in *Metal Clusters in Chemistry* (Eds.: P. Braunstein, L. A. Oro, P. R. Raithby), Wiley-VCH, Weinheim, **1999**, p. 48 – 72; d) M. Veith in *Metal Clusters in Chemistry* (Eds.: P. Braunstein, L. A. Oro, P. R. Raithby), Wiley-VCH, Weinheim, **1999**, p. 73 – 90.

[5] D. M. Mingos, H. R. Powell, T. L. Stolberg, *Transition Met. Chem.* **1992**, *17*, 334 – 337.

[6] Z. Demidowicz, R. L. Johnston, J. C. Machell, D. M. P. Mingos, I. D. Williams, *J. Chem. Soc. Dalton Trans.* **1988**, 1751 – 1756.

[7] W. Clegg, *Acta Crystallogr. Sect. B* **1978**, *34*, 278 – 281.

[8] L. H. Gade, *Eur. J. Inorg. Chem.* **2002**, 1257 – 1268.

[9] M. Contel, K. W. Hellmann, L. H. Gade, I. Scowen, M. McPartlin, *Inorg. Chem.* **1996**, *35*, 3713 – 3715.

[10] B. Findeis, M. Contel, L. H. Gade, M. Laguna, M. C. Gimeno, I. J. Scowen, M. McPartlin, *Inorg. Chem.* **1997**, *36*, 2386 – 2390.

[11] a) *Gold: Progress in Chemistry and Biochemistry and Technology* (Ed.: H. Schmidbaur), Wiley, Chichester, UK, **1999**; b) H. Schmidbaur, *Chem. Soc. Rev.* **1995**, *24*, 391 – 400; c) D. M. Mingos, *J. Chem. Soc. Dalton Trans.* **1996**, 561 – 566.

[12] a) H. Schmidbaur, *Gold. Bull.* **1990**, *23*, 11 – 21; b) P. Pyykkö, *Chem. Rev.* **1997**, *97*, 597 – 636, and references therein.

[13] F. Gabbaï, A. Schier, J. Riede, H. Schmidbaur, *Inorg. Chem.* **1995**, *34*, 3855 – 3856.

[14] F. Gabbaï, S.-C. Chung. A. Schier, S. Krüger, N. Rösch, H. Schmidbaur, *Inorg. Chem.* **1997**, *36*, 5699 – 5705.

[15] F. Demartin, M. Manassero, L. Naldini, R. Ruggeri, M. Sansoni, *J. Chem. Soc. Chem. Commun.* **1981**, 222 – 223.

[16] R. Ahlrichs, M. Bär, M. Häser, H. Horn, C. Kölmel, *Chem. Phys. Lett.* **1989**, *162*, 165 – 169.

[17] P. Pyykkö, *Chem. Rev.* **1988**, *88*, 563 – 594.

[18] O. Treutler, R. Ahlrichs, *J. Chem. Phys.* **1995**, *102*, 346 – 352.

[19] A. D. Becke, *J. Chem. Phys.* **1993**, *98*, 5648 – 5652.

[20] J. P. Perdew, *Phys. Rev. B* **1986**, *33*, 8822 – 8824.

[21] F. Weigend, M. Häser, *Theor. Chim. Acc.* **1997**, *97*, 331 – 340.

[22] TURBOMOLE (auxiliary) basis sets can be retrieved from http://www.turbomole.dea) as cited in A. Schäfer, H. Horn, R. Ahlrichs, *J. Chem. Phys.* **1992**, *97*, 2571 – 2577; b) A. Schäfer, C. Huber, R. Ahlrichs, *J. Chem. Phys.* **1994**, *100*, 5829 – 5835; c) K. Eichkorn, O. Treutler, H. Öhm, M. Häser, R. Ahlrichs, *Chem. Phys. Lett.* **1995**, *240*, 283 – 290; d) K. Eichkorn, F. Weigend, O. Treutler, R. Ahlrichs, *Theor. Chim. Acc.* **1997**, *97*, 119 – 124; e) F. Weigend, H. Patzelt, R. Ahlrichs, *Chem. Phys. Lett.* **1998**, *294*, 143 – 152.

[23] D. Andrae, U. Häußermann, H. Stoll, H. Preuß, *Theor. Chim. Acta* **1990**, *77*, 123 – 141.

[24] A. Schäfer, A. Klamt, D. Sattel, J. C. W. Lohrenz, F. Eckert, *Phys. Chem. Chem. Phys.* **2000**, *2*, 2187 – 2193.

[25] P. Reiß, F. Weigend, R. Ahlrichs, D. Fenske, *Angew. Chem.* **2000**, *112*, 4085 – 4089; *Angew. Chem. Int. Ed.* **2000**, *39*, 3925 – 3929.

[26] The HF wave function was used because it represents the reference wave function for the MP2 calculations.

[27] a) T. McClesky, H. B. Gray, *Inorg. Chem.* **1992**, *31*, 1733 – 1734; b) C. King, J.-C. Wang, M. N. I. Khan, J. P. Fackler Jr. , *Inorg. Chem.* **1989**, *28*, 2145 – 2149; c) C. King, M. N. I. Khan, R. J. Staples, J. P. Fackler Jr. , *Inorg. Chem.* **1992**, *31*, 3236 – 3238; d) V. W.-W. Yam, W.-K. Lee, *J. Chem. Soc. Dalton Trans.* **1993**, 2097 – 2103; e) V. W.-W. Yam, E. C.-C. Cheng, Z.-Y. Zhou, *Angew. Chem.* **2000**, *112*, 1749- 1751; *Angew. Chem. Int. Ed.* **2000**, *39*, 1683 – 1685; f) D. V. Toronto, B. Weissbart, D. S. Tinti, A. J. Balch, *Inorg. Chem.* **1996**, *35*, 2484 – 2489.

[28] Z. Assefa, B. G. McBrunett, R. J. Staples, J. P. Fackler Jr. , B. Assmann, K. Angermaier, H. Schmidbaur, *Inorg. Chem.* **1995**, *34*, 75 – 83.

[29] P. Schwerdtfeger, P. D. W. Boyd, *Inorg. Chem.* **1992**, *31*, 327 – 329.

[30] G. M. Sheldrick, SHELXS-97, Program for Crystal Structure Analysis, University of Göttingen, Göttingen (Germany), **1998**.
[31] G. M. Sheldrick, SHELXL-93, Program for the Refinement of Crystal Structures, University of Göttingen, Göttingen (Germany), **1993**.
[32] X-RED 1.22, STOE Data Reduction Program, Darmstadt, **2001**.
[33] X-SHAPE 1.06, Crystal Optimisation for Numerical Absorption Correction, Darmstadt, **1999**.

